Welding in the World
https://doi.org/10.1007/s40194-024-01855-w

RESEARCH PAPER

Feasibility study on machine learning methods for prediction of process-related parameters during WAAM process using SS-316L filler material

Sharath P. Subadra[1,2] · **Eduard Mayer**[1,2] · **Philipp Wachtel**[1,2] · **Shahram Sheikhi**[1,2]

Received: 15 August 2024 / Accepted: 15 October 2024

Abstract
The geometry of objects by means of wire arc additive manufacturing technology (WAAM) is a function of the quality of the deposited layers. The process parameters variation and heat flow affect the geometric precision of the parts, when compared to the actual dimensions. Therefore, in situ geometry monitoring which is integrated in such a way to enable a backward control model is essential in the WAAM process. In this article, an attempt is made to study the effect of four input variables, namely voltage (U), welding current (I), travel speed and wire feed rate on the output function in the form of two geometrical characteristics of a single weld bead. These output functions which are determinant of the weld quality are width of weld bead (BW) and height of weld bead (BH). A machine learning approach is utilised to predict the bead dimensions based on the input parameters and to predict the parameters by assigning suitable scores. For predicting the bead dimensions, two models, namely linear regression and random forest, shall be utilised, whereas for the purpose of classification based on weld parameters, k-nearest neighbours model shall be employed. Through this work, a wide dataset of parameters in the form of input variable and output in the form bead dimensions are generated for 316LSi filler material which shall be used as a training data for a machine learning algorithm. Subsequently, the predicted parameters shall be cross-checked with actual parameters.

Keywords Wire arc additive manufacturing · 316L steel · Parameters · Weld bead geometry · Machine learning · Predictions

1 Introduction

Wire arc additive manufacturing (WAAM) has emerged as an important additive manufacturing (AM) technology to manufacture large-dimensional components [1]. This AM process has some advantages when compared to other processes including high deposition speed, high material usage efficiency, and inexpensive production and device investment costs [2]. Various arc-based welding processes may serve as the energy source for WAAM. These can be a conventional gas metal arc welding (GMAW) [3], cold metal transfer (CMT) which is a special type of GMAW [4], gas tungsten arc welding (GTAW) [5] and plasma arc welding (PAW) [6]. Due to the poor surface finish, WAAM is usually referred to as being a near-net-shape technique. Therefore, WAAM parts can be used in their as-built conditions as a pedestrian bridge [7] and excavator arm [8]. The application arena can be further widened by employing post-processing in the form of subtractive manufacturing technologies [9].

The choice of material is an important factor, where 316L stainless steel was seen to perform better due to its weldability and corrosion resistance. The material has a wide range of application in the nuclear sector, marine engineering and biomedical implants. Recent studies have focussed on

Recommended for publication by Commission XII-Arc Welding Processes and Production Systems.

✉ Sharath P. Subadra
sharath.peethambaransubadra@haw-hamburg.de

✉ Shahram Sheikhi
shahram.sheikhi@haw-hamburg.de

[1] Institute of Materials Science and Joining Technology, University of Applied Science Hamburg, Berliner Tor 13, 20099 Hamburg, Germany

[2] Forschungs- Und Trasnferzentrum 3I, University of Applied Science Hamburg, Berliner Tor 13, 20099 Hamburg, Germany

Published online: 31 October 2024

analysing the metallurgical characteristics and mechanical properties of 316L thin-walled of thick-walled components from WAAM [10]. Chen et al. [11] found the micro-structural composition dominated by three phases (δ, γ and σ) in which the austenite γ was the most dominant whereas the other two were seen along the grain boundaries. Another study was conducted by Wang et al. [12] along the remelting zone (RZ) and overlapped zone (OZ) of the weld beads along the transversal and building directions. And it was observed that the grains were perpendicular to the fusion lines within RZ and along the build direction in OZ. Thus, this type of epitactic grain growth results in structural anisotropy which is not ideal [13].

The WAAM process presents a few challenges in terms of surface morphology (surface roughness, waviness, defects) and geometrical deviations (layer height and layer width) which limits the use of WAAM from a wide spectrum application within the manufacturing sector. The deposited layers when checked closely consist of peaks and valleys thus increasing surface roughness, and an additional source of material wastage [14]. A control in geometry of the deposited layer is achieved by using multiple CCD cameras. A two-way monitoring via image processing for monitoring geometric parameters such as a layer width, height can save the material by approximately 10% [14]. When printing structures with 316L filler material, the effect of heat input is an important parameter that needs to be controlled and checked. When heat input is increased, the primary dendrite spacing in micro-structures and the corrosion resistance increased, whereas the ferrite content remained the same [15]. Different arc modes (i.e. speed pulse and speed arc) and the different welding-current processes (i.e. speed cold and speed arc) generate different heat input and cooling rates giving rise to in-homogeneity in micro-structure and mechanical properties when using 316L filler material [16].

Process parameters have thus been an important field of research when WAAM is considered, especially the quality of the structure obtained in terms of layer geometry. The relationship between WAAM input parameters and dimensions of the final product is complex and non-linear. There are several ways to overcome this challenge, and among them machine learning (ML) techniques may help it better. In a study conducted by Yaseer et al. [17], two machine learning approaches, namely random forest (RF) and multilayer perception (MLP), were used to optimise the layer roughness. Here, it was concluded that the latter approach outperformed the former. A melt pool depth estimation (MDPE) was proposed using an artificial neural network (ANN) by Jeon et al. [18] to infer the bonding between layers and the melt pool depth. Here, a coaxially aligned infrared camera and a laser line scanner were used to collect the data. Ruchi S et al. [19] in their study examined the effect of parameters (current, travel speed) and layer number on prediction responses using three popular ML techniques, namely RF, k-nearest neighbour (KNN) analysis and support vector regression (SVR). It was concluded that RF model predicts the layer height and width with accuracies nearing 94% and 99% respectively [19]. Therefore, ML techniques can be used to arrive at optimised WAAM parameters to achieve specific mechanical properties or minimise defects.

Though ML techniques have been used widely in the WAAM process, the optimised parameters for different feed materials have not been widely studied especially in the case of 316L stainless steel. While going through the literature, a few that were found are summarised in this paragraph. The geometric structure and quality of a single welding bead (this includes smooth shape, less spatter) play an important role in the final shape of the structure [20]. The travel speed is seen to affect the bead height and width to a larger extent and an optimum parameter affecting the geometry can be estimated using the grey-related analysis (GRA) and techniques for order preferences by similarity-to-ideal solution (TOPSIS) [19]. Back propagating neural networks (BPNN) can predict the bead height and width under different process parameters, where the errors can be as low as 6% [21]. The central angle of bead is an important variable affecting its stability, and if not considered, the bead shape may collapse with increasing number of layers. This can be addressed with the help of a support vector machine classifier (SVM) [21].

This study aims to (i) conduct a set of experiments with different voltage, current and feed rate, thereafter measure the bead width and height. The dataset generated would be used as a training set to train an algorithm, (ii) use three ML techniques, namely linear regression (LR), random forest (RF) and k-nearest neighbour (KNN) classifiers respectively, to check their feasibility and accuracy in predicting the parameters and (iii) select the ideal techniques and test it with test data and hence validating the method.

2 Experimental procedure

2.1 Experimental methodology

The experimental study was conducted using a 316L stainless steel wire of 1 mm diameter as feedstock to deposit on commercial steel plates (S355) of dimensions 250 × 80 × 100 mm. A 6-axis robot arm (KUKA KR 6 R900) was used to deposit the feedstock with an inert metal gas (MIG) power source (Fronius, Model: TPS400i). The shield gas employed consists of 2% CO_2 and 98% argon and the chemical composition of the wire is illustrated in Table 1.

The equipment is as shown in the figure below (Fig. 1) on which a systematic experimental study was conducted by varying input parameters, namely voltage, current, wire

Table 1 Chemical composition of wire (wt. %)

	Cr	Ni	Mo	Mn	Si	C	N	Nb	P	Fe
316L	18.65	11.64	2.29	1.76	0.65	0.026	0.035	0.016	0.003	64.62

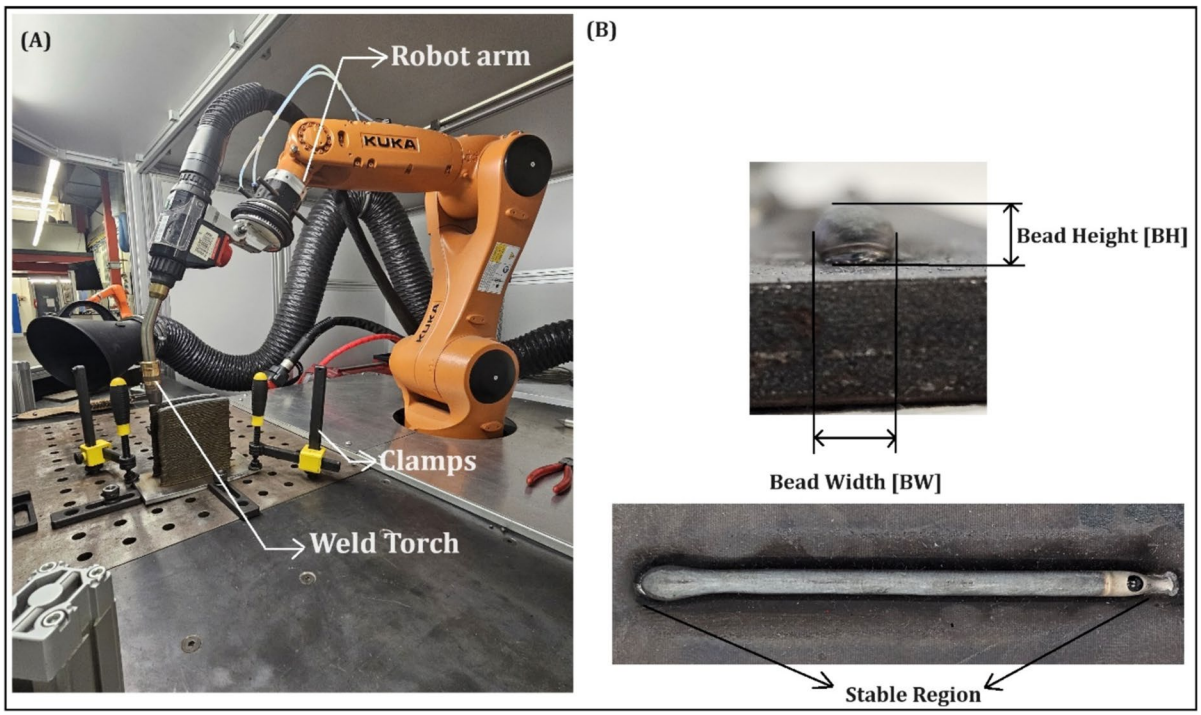

Fig. 1 **A** Experimental setup and **B** bead geometry

feed rate and travel speed. A total of 58 tests were performed to collect information to train an algorithm. The output was recorded in terms of bead height (BH) and bead width (BW) using laser profile scanners from Micro-Epsilon (scanCONTROL 30×0 laser scanner). The wire spool is installed in the wire feeding mechanism to ensure a smooth and consistent feed.

The tests can be classified into seven groups, depending on the travel speed adopted in the study. They are as shown in the table below, where in each group the number of tests varies based on the wire feed rate used. Each feed rate has a pre-set voltage and current set in the power source. The number of feed rate varied in each group and the numbers are mentioned in Table 2. Therefore, a total of 58 tests were carried out and in each test the width and height of the beads were obtained via scanning. While scanning, a total of 94 data points were obtained for width and height respectively, which means while scanning the entire bead length (100 mm) at regular intervals of 1 mm the height and width were obtained.

From the datasets obtained, three machine learning techniques were adopted in this study (LR, RF and KNN), where the former two (LR and RF) will be used to identify "which inputs produce what kind of outputs", where the inputs are travel speed, feed rate, voltage and current, the corresponding outputs being an averaged BW and BH. KNN shall be used to classify weld parameters based on a scoring technique which is elaborated in the next section.

2.2 Machine learning methodology

Three ML models will be studied in this paper, and they are LR, RF and KNN. The first two models shall be used

Table 2 Study groups based on travel speed

Group	Travel speed [mm/min]	Number of tests
A	240	8
B	300	11
C	360	11
D	420	10
E	480	7
F	540	7
G	600	4
	Total tests	58

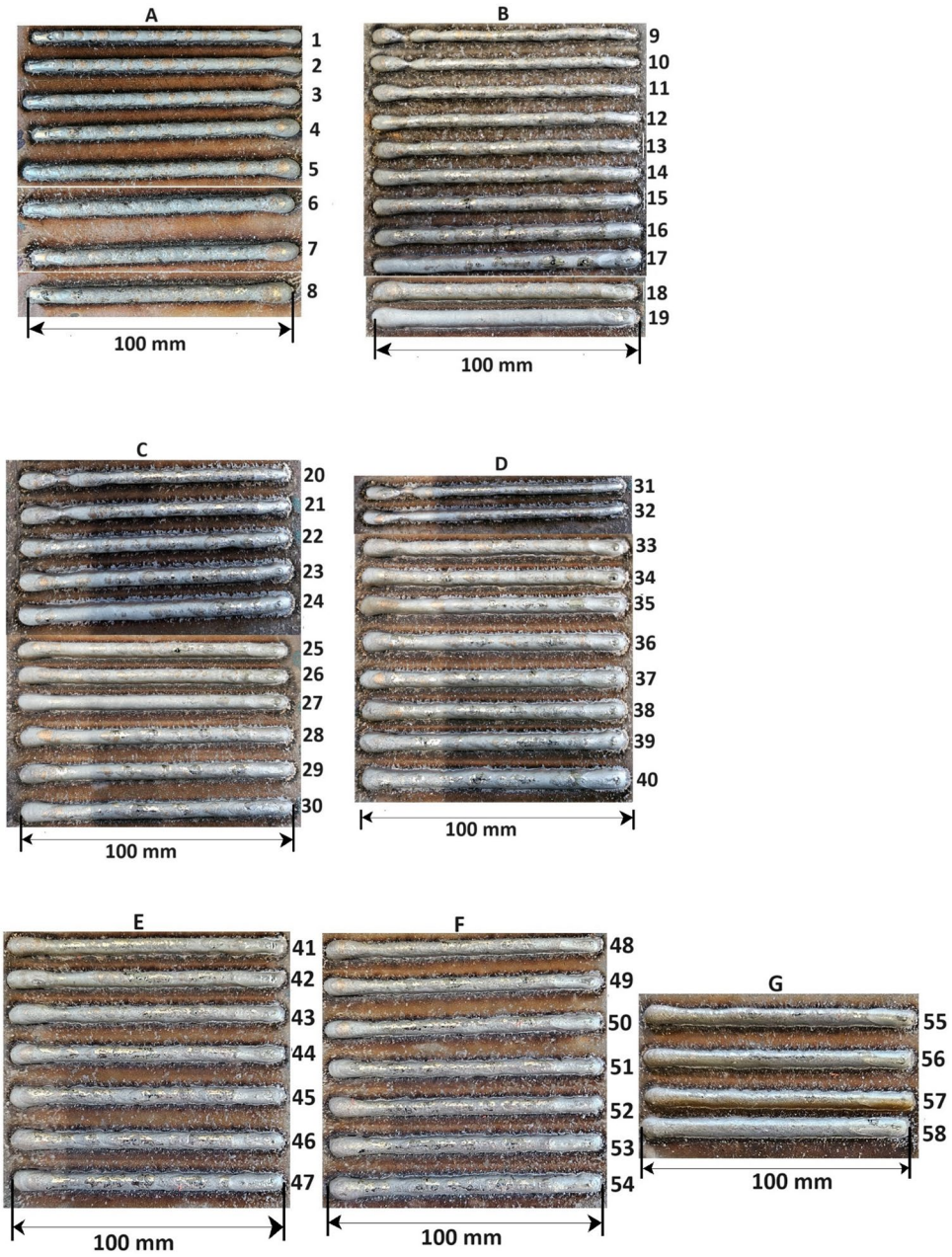

Fig. 2 Seven groups of tests along with the respective weld beads (test groups from **A** to **G**, corresponding to data in Table 2)

for a comparative study to predict the bead geometry (averaged values), while KNN shall be employed to find the best parameters that can be used to carry out a normal WAAM process. Therefore, to make the readers more familiar with the models, a brief description of the three is elaborated below:

A) Linear regression (LR): The method adopted for this study is also termed as multiple linear regression (MLR), which is a statistical technique that uses several explanatory variables to predict the outcome. Here, the explanatory variables are the feed rate, travel speed, voltage and current, whereas the outcome is BH and BW. The formula used for this method is:

$$Y_i = b_o + b_1 X_{i1} + b_2 X_{i2} + \ldots + b_p X_{ip} + \in \quad (1)$$

where for $i = n$ observations:

Y_i is the dependent variable, X_i the explanatory variable, b_o the y-intercept which is a constant term, b_p slope coefficients for each explanatory variable and $\in$ is the models error term [22].

B) Random forest (RF): As opposed to LR where a function can be easily expressed as an equation, RF cannot

be expressed as such. It works based on the concept of decision trees, the inner working of which can be in the form of a bunch of *if-else* conditions. It begins with one node, and this node splits into left and right node decision nodes, and these nodes are further split into their respective right and left nodes. At the end of a leaf node, the averaged observation that occurs within the area is computed. The value in the leaves is normally the averaged observations occurring within the specific region [19].

C) K-nearest neighbour (KNN): This is a popular ML algorithm used for classification and regression. The model predicts the output value of a new observation by taking the average of the k-nearest data points from the training set. The distance between the data points is measured using the Euclidean distance equation:

$$d(X,Y)=\sqrt{\left(\left(X_1-Y_1\right)^2+\left(X_2-Y_2\right)^2+\cdots+\left(X_n-Y_n\right)^2\right)} \quad (2)$$

where X_i and Y_i are the values of the i^{th} feature in data points X and Y, respectively. The k data points in the training set with the smallest distance values are selected as the nearest neighbours once the distance between the new data point and all the data points in the training set has been calculated. Subsequently, the averaged output of the k-nearest neighbours is calculated to the predicted output value. This model is also termed as a non-parametric model owing to very few assumptions that are made in the process. The model is effective even when the data points are limited [19, 23].

This paper intends to use the first two modes (LR and RF) to predict the bead geometries based on a set of input (feed rate, travel speed, volt and current). A comparison shall be

Table 3 Input and output parameters from experiments. *T.S* travel speed, *W.F.R* wire feed rate

	Input				Output			Input				Output	
Sl. No	T.S [m/sec]	W.F.R [m/min]	Volt [V]	Current [A]	BW_n [mm]	BH_n [mm]	Sl. No	T.S [m/sec]	W.F.S [m/min]	Volt [V]	Current [A]	BW_n [mm]	BH_n [mm]
1	0.004	4	11.2	78	3.78	4.015	30	0.006	10.5	16.1	174	5.53	4.31
2	0.004	4.5	11.3	85	3.905	4.205	31	0.007	6	12.8	107	3.151	3.878
3	0.004	5	11.3	92	3.91	4.405	32	0.007	6.5	13	112	3.849	3.805
4	0.004	5.5	11.4	99	4.545	4.57	33	0.007	8	13.7	131	4.327	3.626
5	0.004	6	12.9	107	4.795	4.655	34	0.007	8.5	13.8	140	4.532	3.616
6	0.004	6.5	12.2	110	4.63	4.675	35	0.007	9	15.3	157	4.756	3.791
7	0.004	7	12.6	115	4.925	4.665	36	0.007	9.5	15.2	168	4.803	3.729
8	0.004	7.5	13	120	5.365	5.44	37	0.007	10	15.4	184	5.03	4.058
9	0.005	4	12.3	77	3.75	3.865	38	0.007	10.5	16.5	166	5.195	3.956
10	0.005	4.5	12.5	85	3.85	4.04	39	0.007	11	16.8	173	5.119	3.781
11	0.005	5	12.5	94	3.985	4.03	40	0.007	11.5	17	181	5.465	3.85
12	0.005	5.5	12.6	100	4.105	3.935	41	0.008	9	15.5	151	4.056	3.726
13	0.005	6	13.4	105	4.39	4.095	42	0.008	9.5	15.4	162	4.487	3.903
14	0.005	6.5	13.6	109	4.88	4.16	43	0.008	10	15.7	169	4.775	4.055
15	0.005	7	13.6	114	4.64	3.875	44	0.008	10.5	16.1	173	4.798	4.171
16	0.005	7.5	13.8	121	4.635	3.805	45	0.008	11	16.6	178	4.339	3.93
17	0.005	8	14.3	128	5.48	4.155	46	0.008	11.5	16.6	183	5.101	3.945
18	0.005	8.5	14.3	135	6.015	4.01	47	0.008	12	17	189	5.129	4.021
19	0.005	9	15.6	149	6.05	3.82	48	0.009	10	15.8	170	5.72	3.035
20	0.006	5.5	12.7	103	3.535	3.77	49	0.009	10.5	16	174	5.653	4.44
21	0.006	6	12.7	108	3.685	3.96	50	0.009	11	16.1	181	6.002	4.44
22	0.006	6.5	13.6	112	4.01	3.67	51	0.009	11.5	16.4	186	6.124	4.266
23	0.006	7	13.3	117	4.195	3.785	52	0.009	12	17.1	192	6.267	4.818
24	0.006	7.5	13.9	124	4.14	3.91	53	0.009	12.5	17.3	201	6.956	4.772
25	0.006	8	13.8	127	4.655	3.87	54	0.009	13	18.4	211	7.429	4.677
26	0.006	8.5	14.5	137	4.975	3.845	55	0.01	11.5	16.4	189	4.329	3.422
27	0.006	9	15.2	148	5.23	3.875	56	0.01	12	16.5	194	5.14	3.24
28	0.006	9.5	15.6	160	5.28	4.085	57	0.01	12.5	17.3	204	5.016	3.44
29	0.006	10	15.6	167	5.67	5.598	58	0.01	13	18.2	214	5.719	3.493

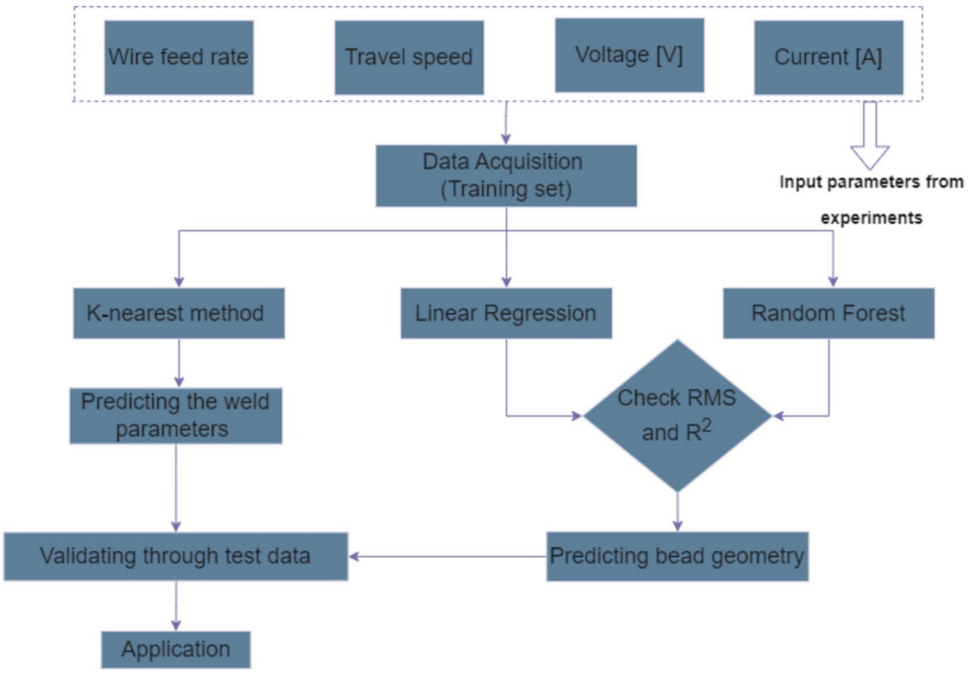

Fig. 3 Flowchart illustrating the general algorithm for predicting weld parameters and bead geometry

made between the two models on their performance by comparing the root mean squared (RMS) value and the coefficient of determination (R^2). The last model shall be used to predict the best parameters based on a scoring system assigned to each weld bead based on their appearance, BW and BH consistency along the whole length. The criteria on which such scores are allotted are described below:

a) If standard deviation of data points collected for BW and BH height along bead length is less than 0.1, in addition to a smooth surface which is not coarse and rough shall be allotted a rank "0".
b) If the standard deviation is between 0.1 and 1, and the appearance of the bead is coarser then a score"1" is allotted.
c) Score "2" is allotted if the standard deviation exceeds 1 and the surface appears very coarse. Thus, from 0 to 2, a score of 0 mean the best and a score of 2 means bad.

All the beads are shown in the figure below (Fig. 2).

3 Results and discussions

Based on the experimental procedure elaborated above, a large amount of dataset was generated for training the ML models. The dataset, since being too large, is condensed and shown in Table 3. The BW and BH for each experiment are shown as BW_n and BH_n where "n" denotes only one data point that is shown in the table, but there were 96 points in total for each of the output parameters.

As against convention, 85% of the data was used to train the three models, and the remaining 15% was used to test the models for their feasibility. As mentioned in the previous section, ML models LR and RF will be employed to predict the average BW and BH based on the learned data, whereas KNN will be used to predict the best performing set of parameters based on a rank assigned to each test. This methodology was explained in the previous section. The flowchart of the general algorithm employed in this study is shown below (Fig. 3).

Initially using the LR and RF models, the bead geometry was tried to predict, and based on which the results are displayed in Fig. 4. Figure 4A and B illustrates results from the LR model, while (C) and (D) from RF model respectively. The blue dots are the actual data from experiments and the orange dots are the predicted values based on the data using which the models were trained. The BW and BH closely aligned with the actual predicted values and to further draw some insight the RMS and R^2 values of the training and test sets were checked, and they are displayed in Table 4. While closely studying Table 4 and Fig. 4, a trend arises where LR seems to predict the outcome better when compared to RM. The MSE in the case of LR was zero which means the predicted values were close to the actual values, whereas in the case of RF it was not the case. Furthermore, R^2 values from LR were as close as to unity as against RF, which further reinforces the argument. While looking into the coloured dots in Fig. 4, the oranges and blues were coincident in (A)

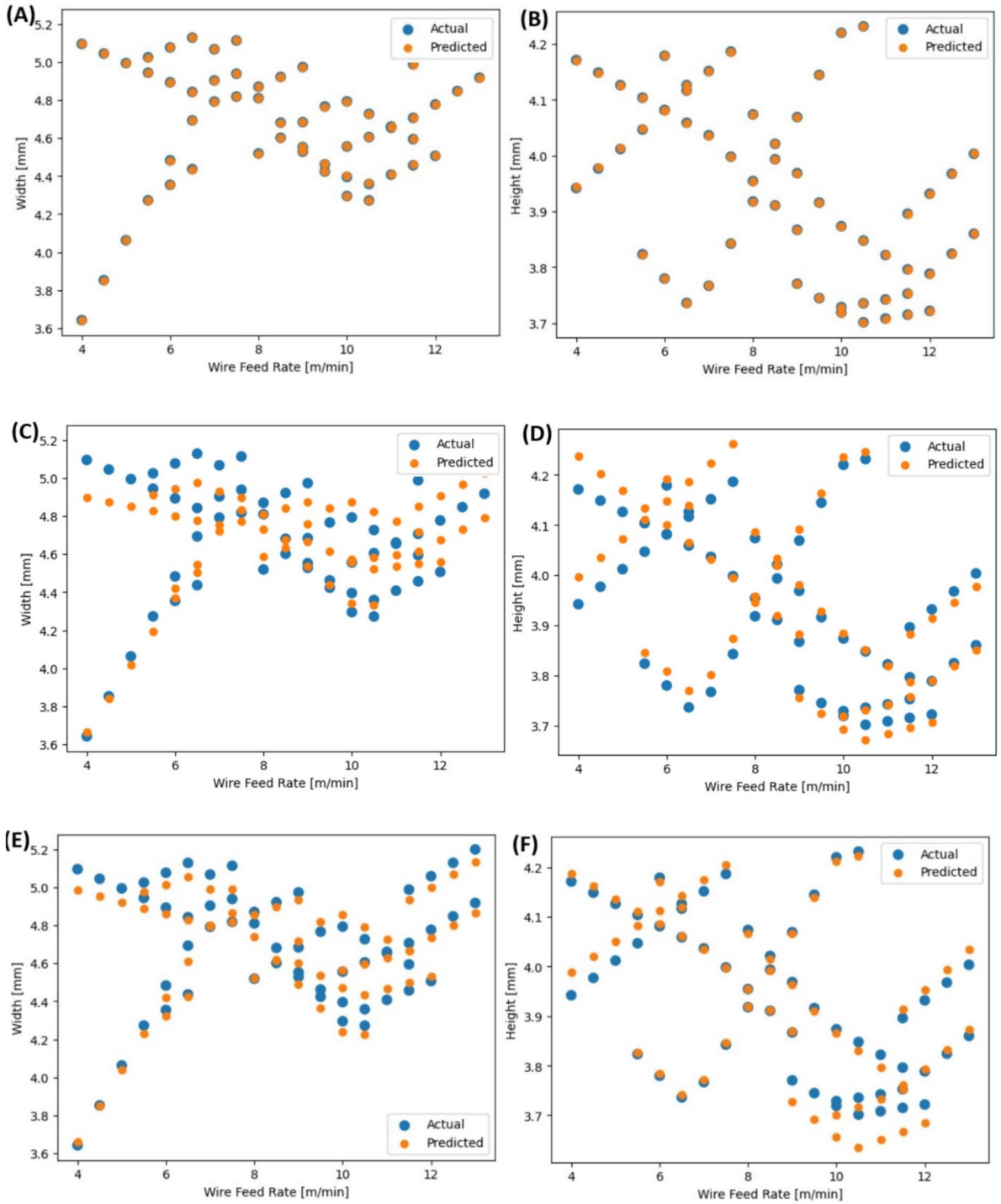

Fig. 4 **A** and **B** Actual and predicted outcomes of width and height from linear regression model. **C** and **D** Actual and predicted outcomes of width and height from random forest model. **E** and **F** Actual and predicted outcomes of width and height from randon forest model post hyperparameter training

and (B) representing LR, and this was not the case in RF seen in (C) and (D).

Further, with respect to RF, there is a wide range of fine tuning options available to make the model more accurate. These are options/process termed as "Hyperparameters tuning", which are settings of an algorithm that can be adjusted to optimise its performance. Also termed as hyperparameters, these should be set before the actual training process.

Table 4 Compilation of MSE and R^2 values for both the models

Model	MSE [Training_set]	R^2 [Training_set]	MSE [Testing_set]	R^2 [Testing_set]
LR	0.0	1	0.00001	0.999999
RF	0.0239	0.9546	0.03489	0.7760

Table 5 Hyperparameter for bead width and bead height

Hyperparameters	For bead width	For bead height
n_estimators	100	72
max_depth	80	None
max_features	2	sqrt
bootstrap	True	False
min_samples_leaf	3	1
min_sample_split	10	2

Table 6 Model performance check based on the *k* factor

k factor	Model score
3	0.7777
4	1
5	1
6	1
7	1
8	0.8888

But, here the RF was trained with default parameters initially, which gave an R^2 value of 0.7760. This necessitated fine tuning with hyperparameters and in the case of random forest this includes the number of decision trees in the forest and the number of features considered by each tree when splitting the node. The sklearn RF's tunable hyperparameters include a number of decision trees (n_estimators), the maximum depth of the decision tree (max_depth), the split criteria (criterion), the minimum of samples for internal node splitting (min_samples_split), the minimum number of samples for leaf nodes (min_samples_leaf), whether bootstrap sampling is used (bootstrap) and the maximum number of features (max_features) [24]. These parameters are optimised using a grid search method. The optimised parameters are shown in Table 5, for both bead width and height with respect to wire feed rate. The RF model was trained again with these respective parameters and Fig. 4E and F shows the outcome. It is clear that the predicted dots moved closer to the actual dots, and as per the seen observations, it can be

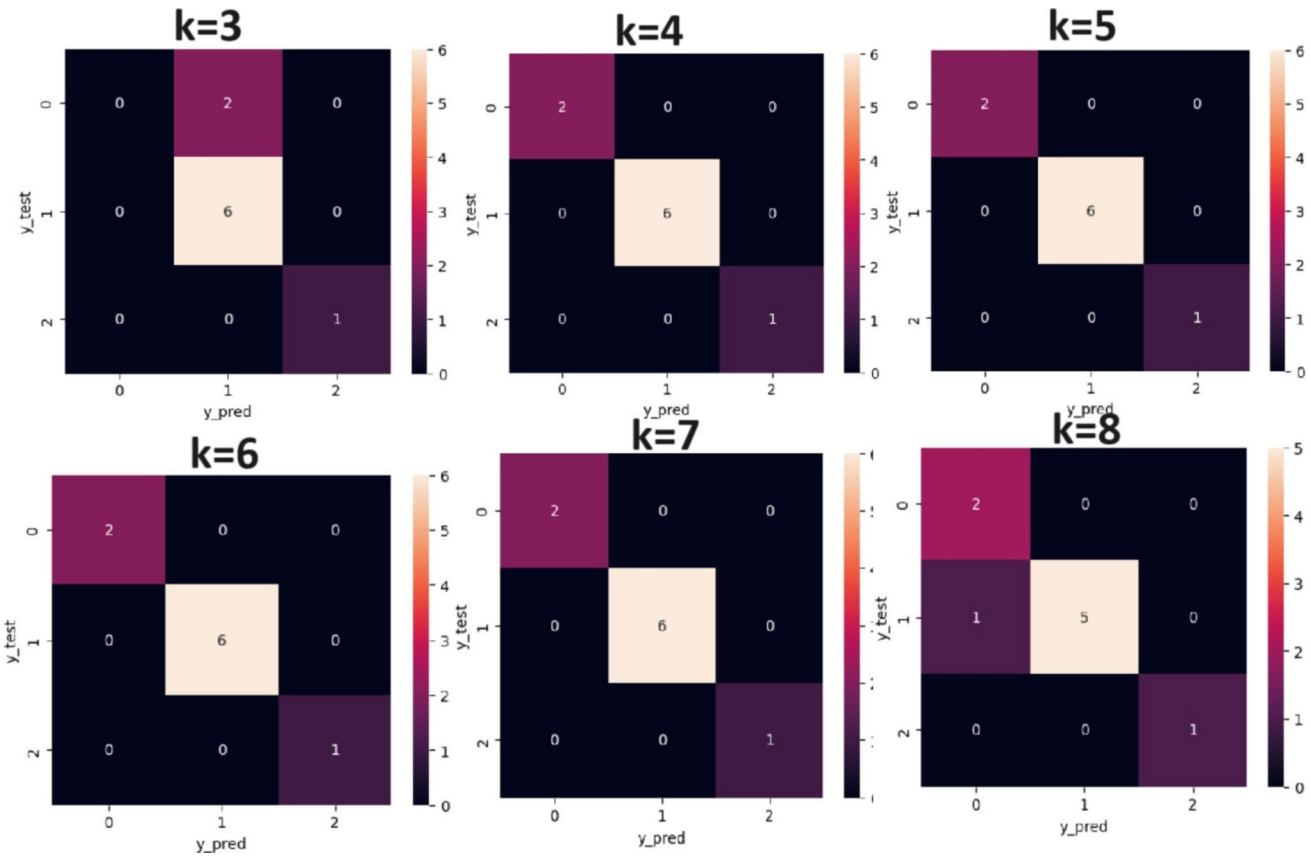

Fig. 5 True and false outcomes for different *k* factors (k=3 until 8)

stated that with more data especially those of temperature along the bead length and cooling rates, RF will better predict the outcome as against a more conventional approach such as LR.

KNN model implementation was carried out to ascertain the weld parameters based on score allotted to each parameter. The methodology was explained earlier, whereas here the results in terms of "*k*" factor are elaborated. The *k* factor was altered between a range of 3 to 8 and the model score checked, and if the score is closer to 1, the better is the model predicting the right outcome. Table 6 illustrates the results in terms of the *k* factor and the model score.

To show the predictability of the knn model based on the *k* factor, a confusion matrix was employed as seen in Fig. 5. A confusion matrix is a better tool that can be used to test the accuracy of classification models such as knn. The correct number of predictions is seen along the diagonals, and anything outside the diagonal is a wrong prediction. From Table 3, there are 57 rows of data, and the total columns in each row was 172. The training set among these data points were 85%, while the rest was used to test the model. Fifteen percent of the rows amount to 8.7 (approx 9), and this is equal to the total number seen in the matrix cells below. Therefore, when a *k* factor of 3 was used, the model predicted seven times the right outcome. Six times score "1" and one time score "2" whereas score "0" was wrongly predicted two times. But when the *k* factor is changed to 4 all the outcomes were correctly predicted and hence all the cells are zero except the diagonals. The same was true until a *k* factor of 7, but when *k* was 8, score "1" was wrongly predicted as score "0". Thus, arriving at the right *k* factor is important to reduce the amount of wrong predictions.

4 Conclusions

The paper attempts to study the ability of three machine learning models for WAAM, namely, linear regression (LR), random forest (RF) and k-nearest neighbours (KNN) in predicting the weld geometry and the weld parameters respectively. The following can be concluded from this study:

a) From LR and RF, the former was able to rightly predict the outcome based on travel speed, wire feed rate, voltage and current. This was clarified by checking three aspects of the outcome, namely, the RMS value, the R^2 value and plots of the actual and predicted values. The RMS was seen as zero in the case of LR thus, implying that the predicted outcome matches that of the actual outcome, whereas in the case of RF, a slight deviation was seen in RMS implying non-consistent predicted outcomes.

b) When KNN model was used to correctly predict weld parameters based on a scoring system, it was seen that correct *k* factors need to be ascertained. A *k* factor between 4 and 7 correctly classified the experiments based on the weld parameters while anything below 4 and above 7 was seen to reduce the effectiveness of the model. A confusion matrix was employed to check the effectiveness of the model.

Further, the study aims to use the parameters to print a set of walls of specified dimensions. Subsequently, specimens shall be cut and milled to precision from these walls to conduct tension test, along with quality tests in terms of porosity within the structure.

Abbreviations *WAAM*: Wire arc additive manufacturing; *BW*: Bead width; *BH*: Bead height; *AM*: Additive manufacturing; *GMAW*: Gas metal arc welding; *CMT*: Cold metal transfer; *GTAW*: Gas tungsten arc welding; *PAW*: Plasma arc welding; *RZ*: Remelting zone; *OZ*: Overlapped zone; *ML*: Machine learning; *MLP*: Multi-layer perception; *RF*: Random forest; *MDPE*: Melt pool depth estimation; *ANN*: Artificial neural network; *KNN*: K-nearest neighbour; *SVR*: Support vector regression; *BPNN*: Back propagating neural networks; *SVM*: Support vector machine classifier; *LR*: Linear regression; *MIG*: Metal inert gas; *MLR*: Multiple linear regression; *RMS*: Root mean square; *TS*: Travel speed; *WFR*: Wire feed rate

Acknowledgements Mr. Sven Trapp and Mr. Thomas Hilbrecht, University of Applied Science Hamburg, Institute of Material Science and Joining, Berliner Tor 13, D-20099, Germany.

Funding Open Access funding enabled and organized by Projekt DEAL. This is a part of a research project "LAYER" with nine cooperative partners, namely Mecklenburger Metallguss GmbH, MEYER WERFT GmbH & Co. KG, Laser cladding Germany GmbH, FEM-Composites GmbH, Ing. Grimm Schweißtechnik GmbH, HiFIT Vertriebs GmbH, KARSTENS WATERCUT & WELDING, TRIMET Aluminium SE, Deutsches Zentrum für Luft- und Raumfahrt e,V.-Institut für Maritime Energiesystem (DLR MS). The project is funded by Forschungszentrum Jülich GmbH and Bundesministerium für Wirtschaft und Klimaschutz.

Data availability The data will be available on demand.

Declarations

Conflict of interest The authors declare no competing interests.

References

1. Jafari D, Vaneker THJ, Gibson I (2021) Wire and arc additive manufacturing: opportunities and challenges to control the quality and accuracy of manufacturing parts. Mater. Des. 202:109471 ([1 in 8])
2. Pattanayak S, Sahoo SK (2021) Gas metal arc welding based additive manufacturing-a review. CIRP J Manuf Sci Technol 33:398–441 ([2 in 8])
3. Le VT, Mai DS, Hoang QH (2020) A study on wire and arc additive manufacturing of low-carbon steel components: process stability, microstructural and mechanical properties. J Braz Soc Mech Sci Eng 42:480
4. Aldalur E, Suárez A, Veiga F (2021) Metal transfer modes for wire arc additive manufacturing Al-Mg alloys: Influence of heat input in microstructure and porosity. J Mater Process Technol 297:117271
5. Yilmaz O, Ugla AA (2017) Microstructure characterization of SS308LSi components manufactured by GTAW-based additive manufacturing: shaped metal deposition using pulsed current arc. Int J Adv Manuf Technol 89:13–25
6. Bai X, Colegrove P, Ding J, Zhou X, Diao C, Bridgeman P et al (2018) Numerical analysis of heat transfer and fluid flow in multilayer deposition of PAW-based wire and arc additive manufacturing. Int J Heat Mass Transf 124:504–516
7. Gardner L, Kyvelou P, Herbert G, Buchanan C (2020) Testing and initial verification of the world's first metal 3D printed bridge. J Constr Steel Res 172:106233
8. Greer C et al (2019) Introduction to the design rules for metal big area additive manufacturing. Addit Manuf 27:159–166
9. Ma G et al (2019) Optimization strategies for robotic additive and subtractive manufacturing of large and high thin-walled aluminium structures. Int J Adv Manuf Technol 101:1275–1292
10. Jin W, Zhang C, Jin S, Tian Y, Wellmann D, Liu W (2020) Wire arc additive manufacturing stainless steels: a review. Appl Sci
11. Chen X et al (2017) Microstructure and mechanical properties of the austenitic stainless steel 316L fabricated by gas metal arc additive manufacturing. Mater Sci Eng A 703:567–577
12. Wang C et al (2020) Study on microstructure and tensile properties of 316L stainless steel fabricated by CMT wire and arc additive manufacturing. Mater Sci Eng A 796:14006
13. Wu W et al (2019) Forming process, microstructure, and mechanical properties of thin-walled 316L stainless steel using speed-cold-welding additive manufacturing. Metals 9:109
14. Derekar KS (2018) A review of wire arc additive manufacturing and advances in wire arc additive manufacturing of aluminium. Mater Sci Technol 34:895–916
15. Wen DX et al (2020) Effects of linear heat input on microstructure and corrosion behaviour of austenitic stainless steel processed by wire arc additive manufacturing. Vacuum 173:109131
16. Wang L et al (2019) Correlation between arc mode, microstructure, and mechanical properties during wire arc additive manufacturing of 316L stainless steel. Mater Sci Eng A 751:183–190
17. Yaseer A, Chen H (2021) Machine learning based layer roughness modelling in robotic additive manufacturing. J Manuf Process 70:543–552
18. Jeon I, Yang L, Ryu K, Sohn H (2021) Online melt pool depth estimation during directed energy deposition using coaxial infrared camera, laser line scanner, and artificial neural network. Addit Manuf 47:102295
19. Sharma R et al (2023) Forecasting of process parameters using machine learning techniques for wire arc additive manufacturing process. Materials Today: Proceedings 80:248–253
20. Le VT et al (2022) Prediction and optimization of processing parameters in wire and arc-based additively manufacturing of 316L stainless steel. J Braz Soc Mech Sci Eng 44:394
21. Kim DO, Lee CM, Kim DH (2024) Determining optimal bead central angle by applying machine learning to wire arc additive manufacturing (WAAM). Heliyon 10:e23372
22. Dutta P, Pratihar DK (2007) Modeling of TIG welding process using conventional regression analysis and neural network-based approaches. J of Mat Proc Technol 184:56–68
23. Vincent A, Natarajan H. Machine learning approach to predict bead height and width in wire arc additive manufacturing sample. In: International conference on advances in design, materials, manufacturing and surface engineering for mobility. https://doi.org/10.4271/2023-28-0145
24. Zhu N, Zhu C, Zhou L, Zhu Y, Zhang X (2022) Optimization of the random forest hyperparameters for power industrial control systems intrusion detection using an improved grid search algorithm. Appl Sci 12(20):10456